Int. J. Anal. Appl. (2023), 21:110

International Journal of Analysis and Applications

A Novel Approach for Digital Image Compression in Some Fixed Point Results on Complete $G-$metric Space Using Comparison Function

R. Anna Thirumalai, S. Thalapathiraj*

Department of Mathematics, Faculty of Engineering and Technology, SRM Institute of Science and Technology, Vadapalani Campus, No.1 Jawaharlal Nehru Salai, Vadapalani, Chennai-600026, Tamil Nadu, India

**Corresponding author:* thalapas@srmist.edu.in

Abstract. In the present time world, digital images are crucial for various applications, that includes the medical industry, aircraft and satellite imaging, underwater imaging and so on. For this huge quantities of digital images are produced and used by these applications. For a variety of reasons, these images also need to be transmitted and stored. Therefore, a technique known as compression is applied to resolve this storage issue while transmitting these images. In this article, by extending some unique fixed point theorem results for comparison function on a complete symmetric G-metric space are used and it is a new approach. Moreover, this paper focuses on a compression method using the new structure of extended G-contraction mapping as it assists in compressing the size of the image. Thus, grayscale images are compressed using extended G-contraction mapping. And thus, grayscale images can be represented as matrices in this structure (pixel values). Also, similar images of reduced size can be obtained using an appropriate matrix G-metric and extended G-contraction mapping. The size of the matrix can be substantially reduced without losing any quality by controlling the order of sub matrices. These images are easy to store and transmit, with little variation between the original and contracted image.

1. Introduction

Fixed point theory in metric space is one of the primary research areas in applied and pure mathematics. Its applications are useful in most other areas in various parts of science and engineering. The Banach contraction mapping concept [1], is an important tool in analysis, and also one of the

Received: Mar. 16, 2023.

2020 *Mathematics Subject Classification.* 47H10, 54H25.

Key words and phrases. comparison function; fixed point; extended G-contraction mapping; G-Cauchy sequence; G-metric space; matrix distance.

https://doi.org/10.28924/2291-8639-21-2023-110
ISSN: 2291-8639

fixed point theory's most basic and important results to be considered. Throughout the years, mathematicians have generalized this concept in various approaches and in different spaces. On the other hand, in metric spaces with partial ordering, fixed point theory has drawn a lot of research. (Ran and Reurings, 2004) provided the first finding in this direction and demonstrated applications of their discoveries to matrix equations [21]. There was various generalization of a metric, notably a 2-metric, a D-metric, a G-metric, a cone metric, and a complex-valued metric.

In [2], Gähler first proposed the idea of a 2-metric. Consider a 2-metric is not a continuous function of its variables compared to a standard metric. The results obtained in 2-metric spaces and metric spaces could not then easily relate to one another. The fixed point theorems on 2-metric spaces and metric spaces may be readily unconnected. Due to this, Dhage proposed the idea of a D-metric in [3]. However, Mustafa and Sims demonstrated in [4] found that most of the topological characteristics of the D-metric were incorrect. To overcome the drawbacks of a D-metric, Mustafa and Sims established the idea of a G-metric in [5]. The authors analyzed the topological characteristics of this space and demonstrated how G-metric spaces can use the analogue of the Banach contraction mapping concept and numerous fixed point theorems on G-metric spaces have been established since then. The concept of a cone metric was defined by Huang and Zhang in [7]. Subsequently, many authors developed numerous fixed point theorems from metric spaces to cone metric spaces. The fixed point results in cone metric spaces can also be obtained by reducing cone metric spaces to their standard metric counterparts. And, it was also demonstrated by various authors. Azam, Fisher, and Khan [8] demonstrated the concept of a complex-valued metric and stated some fixed point theorems.

A digital image is made up of a number of pixels, each of which has a unique position and value. Mathematical representations of these images are achievable. These are also referred to as raster images or bitmap images. Due to its numerous uses in various industries, digital imaging is in high demand. The drawbacks of digital images are that they require more memory space and consequently take a longer time to transfer from one device to another. Therefore, the size of the image is crucial in these situations in order to get better outcomes. A contraction is a tool that reduces the length of a distance, and it is at the centre of a wide range of image processing tools. Using general topology and functional analysis, digital topology is linked to the 2D and 3D features of digital images in [18, 26]. In [9–11, 17], Rosenfeld, Kong, Boxer, Karaca, Han, and others have used topological tools, particularly algebraic topology, to characterize the properties of digital images.

In [9], Rosenfeld found that the field of digital topology has influenced a wide range of uses, including pattern recognition and image processing. The concept of digital continuity for 2D and 3D digital images is being further developed in [33, 40]. In [19–21], Boxer studied a variety of continuous digital functions as well as the digital version of several topological concepts. In [11, 12], Ege et al. explored the Banach fixed point theorem as it is pertinent to digital images. Therefore, introduced different outcomes and characteristics on 2D digital homology groups, proved the Lefschetz fixed point theorem for digital images in [11], gave some examples of the fixed point property, and illustrated that sphere-like digital images have the fixed point property. By implementing the Banach contraction principle to digital metric spaces at digital intervals, simply closed k-curves, and simply closed 18-surfaces, in [10, 13] Sang-Eon Han illustrated in the digital metric space which is complete. The need for storage space is growing in combination with the rapid demand for large amounts of image files. There are different kinds of compression methods available to help in reducing the size of these data files. Hence, in this paper, an image contraction approach is used to decrease the dimension of image files in extended G-contractive mapping applications. Image resizing (decrease) can be accomplished by reducing the total number of pixels.

2. Basic Concepts

Definition 2.1. *[5] Let $\mathcal{X}$ be a non empty set, and let $G : \mathcal{X} \times \mathcal{X} \times \mathcal{X} \to R^+$ be a function satisfying the following conditions:*
(1) $G(x, y, z) = 0$ *if* $x = y = z$
(2) $G(x, x, y) > 0$*; for all* $x, y \in \mathcal{X}$ *with* $x \neq y$
(3) $G(x, x, y) \leq G(x, y, z)$ *for all* $x, y, z \in \mathcal{X}$ *with* $y \neq z$
(4) $G(x, y, z) = G(x, z, y) = G(y, z, x) = \dots$ *(symmetry in all three variables)*
(5) $G(x, y, z) \leq G(x, a, a) + G(a, y, z)$ *for all* $x, y, z, a \in \mathcal{X}$ *(rectangle inequality)*
Then the function G is called a generalized metric or more specially, a G-metric on $\mathcal{X}$*, and* $(\mathcal{X}, G)$ *is called a G-metric space.*

Definition 2.2. *[5] Let* $(\mathcal{X}, G)$ *be a G-metric space.*
(i) *The sequence* $\{x_n\}$ *is G-convergent to* $x \in \mathcal{X}$ *if and only if* $\lim_{n,m\to\infty} G(x, x_n, x_m) = 0$.
(ii) *The sequence* $\{x_n\}$ *is G-Cauchy if and only if* $\lim_{n,m,l\to\infty} G(x_n, x_m, x_l) = 0$.
(iii) $(\mathcal{X}, G)$ *is G-complete if and only if every G-Cauchy sequence in* $\mathcal{X}$ *is G-convergent.*

Definition 2.3. *[27, 28]A map* $\varphi : [0, \infty) \to [0, \infty)$ *is called comparison function if it satisfies:*
(i) φ *is monotonic increasing.*
(ii) *The sequence* $\{\varphi^n(t)\}_{n=0}^{\infty}$ *converges to zero for all* $t > 0$.
(iii) $\sum_{k=0}^{\infty} \varphi^k(t)$ *converges for all* $t \in R^+$.

Lemma 2.1. *[27, 28] If* $\varphi : [0, \infty) \to [0, \infty)$ *is called comparison function, then:*
(i) *Each iterate* φ^n *is also comparison function.*
$(ii)\varphi(t) < t$ *for all* $t > 0$.
$(iii)\varphi$ *is continuous at* $t = 0$ *and* $\varphi(0) = 0$.⌋

Definition 2.4. *The matrix* $\mathcal{A}$ *is given by Frobenius norm as:*

$$\rho_F = \sqrt{\sum_{i=1}^{m}\sum_{j=1}^{n}(a_{ij})^2} = \sqrt{trace(\mathcal{A}\mathcal{A}')}$$

3. Main Results

Theorem 3.1. *In a complete symmetric G-metric space $(\mathcal{X}, G)$, a self mapping $\mathcal{T} : \mathcal{X} \to \mathcal{X}$ has a unique fixed point if there exists a comparison function with for all $x, y, z \in \mathcal{X}$, and*

$$\begin{aligned}\varphi(G(\mathcal{T}x,\mathcal{T}y,\mathcal{T}z)) \leq \alpha\varphi(G(x,y,z)) + \beta\varphi\left(\max\left\{G(x,\mathcal{T}x,\mathcal{T}x), G(x,y,z)\right\}\right) \\ + \gamma\varphi\left(\left\{\frac{G(x,y,z)\left[1+\sqrt{G(x,\mathcal{T}x,\mathcal{T}x).G(x,y,z)}\right]^2}{[1+G(x,y,z)]^2}\right\}\right)\end{aligned} \tag{3.1}$$

where $\alpha, \beta, \gamma \in [0,1)$ and $0 \leq \mathcal{L} = \alpha + \beta + \gamma < 1$.

Proof. Let $u_0 \in \mathcal{X}$ be a arbitrary point and the sequence $\{u_n\}$ in $\mathcal{X}$, define as follows

$$u_{n+1} = \mathcal{T}u_n, \quad n = 0, 1, 2, 3.... \tag{3.2}$$

Consider, $\varphi(G(u_n, u_{n+1}, u_{n+1})) = \varphi(G(\mathcal{T}u_{n-1}, \mathcal{T}u_n, \mathcal{T}u_n))$

$$\begin{aligned}\varphi(G(u_n,u_{n+1},u_{n+1})) &\leq \alpha\varphi(G(u_{n-1},u_n,u_n)) + \beta\varphi\left(\max\{G(u_{n-1},\mathcal{T}u_{n-1},\mathcal{T}u_{n-1}), G(u_{n-1},u_n,u_n)\}\right) \\ &\quad + \gamma\varphi\left(\left\{\frac{G(u_{n-1},u_n,u_n)\left[1+\sqrt{G(u_{n-1},\mathcal{T}u_{n-1},\mathcal{T}u_{n-1}).G(u_{n-1},u_n,u_n)}\right]^2}{[1+G(u_{n-1},u_n,u_n)]^2}\right\}\right) \\ &\leq \alpha\varphi(G(u_{n-1},u_n,u_n)) + \beta\varphi\left(\max\{G(u_{n-1},u_n,u_n), G(u_{n-1},u_n,u_n)\}\right) \\ &\quad + \gamma\varphi\left(\left\{\frac{G(u_{n-1},u_n,u_n)\left[1+\sqrt{G(u_{n-1},u_n,u_n).G(u_{n-1},u_n,u_n)}\right]^2}{[1+G(u_{n-1},u_n,u_n)]^2}\right\}\right) \\ &= \alpha\varphi(G(u_{n-1},u_n,u_n)) + \beta\varphi(G(u_{n-1},u_n,u_n)) + \gamma\varphi(G(u_{n-1},u_n,u_n)) \\ \varphi(G(u_n,u_{n+1},u_{n+1})) &\leq (\alpha+\beta+\gamma)\varphi(G(u_{n-1},u_n,u_n))\end{aligned}$$

Since, $\varphi(t) \leq t$, for all $t \geq 0$

$$G(u_n, u_{n+1}, u_{n+1}) \leq \mathcal{L}G(u_{n-1}, u_n, u_n)$$

Continuing in the similar fashion, we have

$$G(u_n, u_{n+1}, u_{n+1}) \leq \mathcal{L}^n G(u_0, u_1, u_1) \tag{3.3}$$

Taking limit $n \to \infty$, $\mathcal{L}^n \to 0$.

$$\lim_{n\to\infty} G(u_n, u_{n+1}, u_{n+1}) = 0 \tag{3.4}$$

For $n > m \geq 1$, then

$$\begin{aligned} G(u_n, u_m, u_m) &\leq G(u_{n-1}, u_n, u_n) + G(u_{n-2}, u_{n-1}, u_{n-1}) + ... + G(u_m, u_{m+1}, u_{m+1}) \\ &\leq \mathcal{L}^{n-1} G(u_0, u_1, u_1) + \mathcal{L}^{n-2} G(u_0, u_1, u_1) + ... + \mathcal{L}^m G(u_0, u_1, u_1) \\ &\leq (\mathcal{L}^{n-1} + \mathcal{L}^{n-2} + ... + \mathcal{L}^m) G(u_0, u_1, u_1) \\ G(u_n, u_m, u_m) &\leq \frac{\mathcal{L}^n}{(1-\mathcal{L})} G(u_0, u_1, u_1) \end{aligned}$$

Taking limit $n, m \to \infty$, we have

$$\lim_{n,m\to\infty} G(u_n, u_m, u_m) = 0. \tag{3.5}$$

To prove: $\{u_n\}$ is Cauchy Sequence

$$G(u_n, u_m, u_l) \leq G(u_n, u_m, u_m) + G(u_m, u_m, u_l)$$

Applying limit $n, m, l \to \infty$, we get

$$\lim_{n,m,l\to\infty} G(u_n, u_m, u_l) = 0 \quad (by\ using\ (3.5)) \tag{3.6}$$

Hence, $\{u_n\}$ is a G-Cauchy sequence.
Since, $(\mathcal{X}, G)$ be G-complete, there exists $p \in \mathcal{X}$ such that,

$$p = \lim_{n\to\infty} u_n. \tag{3.7}$$

Suppose that $\mathcal{T}p \neq p$

$$\begin{aligned} \varphi(G(p, \mathcal{T}p, \mathcal{T}p)) &\leq \varphi(G(p, u_n, u_n)) + \varphi(G(u_n, \mathcal{T}p, \mathcal{T}p)) \\ &\leq \varphi(G(p, u_n, u_n)) + \alpha\varphi(G(u_{n-1}, p, p)) + \beta\varphi\left(\max\{G(u_n, \mathcal{T}p, \mathcal{T}p), G(u_{n-1}, p, p)\}\right) \\ &+ \gamma\varphi\left(\left\{\frac{G(u_{n-1}, p, p)\left[1 + \sqrt{G(u_n, \mathcal{T}p, \mathcal{T}p).G(u_{n-1}, p, p)}\right]^2}{[1 + G(u_{n-1}, p, p)]^2}\right\}\right) \end{aligned}$$

Taking limit $n \to \infty$, we get

$$\varphi(G(p, \mathcal{T}p, \mathcal{T}p)) \leq 0 + \alpha\varphi(0) + \beta\varphi \max\{G(p, \mathcal{T}p, \mathcal{T}p), 0\} + \gamma\varphi\left(\left\{\frac{(0)\left[1 + \sqrt{(G(p, \mathcal{T}p, \mathcal{T}p).0)}\right]^2}{[1+0]^2}\right\}\right)$$

Since, $\varphi(t) \leq t$, for all $t \geq 0$.

$$G(p, \mathcal{T}p, \mathcal{T}p) \leq \beta G(p, \mathcal{T}p, \mathcal{T}p)$$

which is contradiction, since $\beta < 1$

$$Hence,\ \mathcal{T}p = p \tag{3.8}$$

Suppose that $\mathcal{T}p = p$ and $\mathcal{T}q = q$ then by (3.1), we have

$$\begin{aligned}
\varphi(G(p,q,q)) &= \varphi(G(\mathcal{T}p,\mathcal{T}q,\mathcal{T}q)) \\
&\leq \alpha\varphi(G(p,q,q)) + \beta\varphi\left(\max\{G(p,\mathcal{T}p,\mathcal{T}p), G(p,q,q)\}\right) \\
&+ \gamma\varphi\left(\left\{\frac{G(p,q,q)\left[1+\sqrt{(G(p,\mathcal{T}\mathcal{T}p,\mathcal{T}p).G(p,q,q))}\right]^2}{[1+G(p,q,q)]^2}\right\}\right) \\
&= \alpha\varphi(G(p,q,q)) + \beta\varphi\left(\max\{0, G(p,q,q)\}\right) + \gamma\varphi\left(\left\{\frac{G(p,q,q)\left[1+\sqrt{(0).G(p,q,q)}\right]^2}{[1+G(p,q,q)]^2}\right\}\right) \\
&\leq \alpha\varphi(G(p,q,q)) + \beta\varphi(G(p,q,q)) + \gamma\varphi(G(p,q,q)) \\
\varphi(G(p,q,q)) &\leq (\alpha+\beta+\gamma)\varphi(G(p,q,q))
\end{aligned}$$

Since, $\varphi(t) \leq t$, for all $t \geq 0$.

$$G(p,q,q) \leq \mathcal{L}G(p,q,q)$$

which is contradiction, since $\mathcal{L} < 1$

$$p = q \tag{3.9}$$

Thus, $\mathcal{T}$ has a unique fixed point in $\mathcal{X}$. □

Corollary 3.1. *In a complete symmetric G-metric space $(\mathcal{X}, G)$, a self mapping $\mathcal{T} : \mathcal{X} \to \mathcal{X}$ has a unique fixed point if there exists a comparison function with for all $x, y \in \mathcal{X}$, and*

$$\begin{aligned}
\varphi(G(\mathcal{T}x,\mathcal{T}y,\mathcal{T}x)) &\leq \alpha\varphi(G(x,y,x)) + \beta\varphi\left(\max\left\{G(x,\mathcal{T}x,\mathcal{T}x), G(x,y,x)\right\}\right) \\
&+ \gamma\varphi\left(\left\{\frac{G(x,y,x)\left[1+\sqrt{G(x,\mathcal{T}x,\mathcal{T}x).G(x,y,x)}\right]^2}{[1+G(x,y,x)]^2}\right\}\right)
\end{aligned} \tag{3.10}$$

where $\alpha, \beta, \gamma \in [0, 1)$ and $0 \leq \mathcal{L} = \alpha + \beta + \gamma < 1$.

Proof. Put $x = z$, we get the conclusion by using Theorem 3.1. □

Theorem 3.2. *In a complete symmetric G-metric space $(\mathcal{X}, G)$, a self mapping $\mathcal{T} : \mathcal{X} \to \mathcal{X}$ has a unique fixed point and also $\{u_n\}$ converging to a point $p \in \mathcal{X}$ if there exists a comparison function and $\{u_n\}$ has a subsequence converging to a point $p \in \mathcal{X}$ with for all $x, y, z \in \mathcal{X}$,*

$$\begin{aligned}
\varphi(G(\mathcal{T}x,\mathcal{T}y,\mathcal{T}z)) &\leq \alpha\varphi(G(x,y,z)) + \beta\varphi\left(\max\left\{G(x,\mathcal{T}x,\mathcal{T}x), G(x,y,z)\right\}\right) \\
&+ \gamma\varphi\left(\left\{\frac{G(x,y,z)\left[1+\sqrt{G(x,\mathcal{T}x,\mathcal{T}x).G(x,y,z)}\right]^2}{[1+G(x,y,z)]^2}\right\}\right)
\end{aligned} \tag{3.11}$$

where $\alpha, \beta, \gamma \in [0, 1)$ and $0 \leq \mathcal{L} = \alpha + \beta + \gamma < 1$.

Proof. Let $u_0 \in \mathcal{X}$ be a arbitrary point and the sequence $\{u_n\}$ in $\mathcal{X}$, define as follows

$$u_{n+1} = \mathcal{T}u_n, n = 0, 1, 2, 3, \ldots. \tag{3.12}$$

$$If \lim_{k\to\infty} u_{n_k} = p \tag{3.13}$$

Suppose that $\mathcal{T}p \neq p$

$$\begin{aligned}\varphi(G(p, \mathcal{T}p, \mathcal{T}p)) &\leq \varphi(G(p, u_{n_k}, u_{n_k})) + \varphi(G(u_{n_k}, \mathcal{T}p, \mathcal{T}p)) \\ &\leq \varphi(G(p, u_{n_k}, u_{n_k})) + \alpha\varphi(G(u_{n_k-1}, p, p)) + \beta\varphi\left(\max\{G(u_{n_k-1}, \mathcal{T}p, \mathcal{T}p), G(u_{n_{k-1}}, p, p)\}\right) \\ &+ \gamma\varphi\left(\left\{\frac{G(u_{n_k-1}, p, p)\left[1 + \sqrt{G(u_{n_k-1}, \mathcal{T}p, \mathcal{T}p).G(u_{n_k-1}, p, p)}\right]^2}{[1 + G(u_{n_k-1}, p, p)]^2}\right\}\right)\end{aligned}$$

Taking limit $k \to \infty$, we get

$$\varphi(G(p, \mathcal{T}p, \mathcal{T}p)) \leq 0 + \alpha\varphi(0) + \beta\varphi\left(\max\{G(p, \mathcal{T}p, \mathcal{T}p), 0\}\right) + \gamma\varphi\left(\left\{\frac{(0)\left[1 + \sqrt{(G(p, \mathcal{T}p, \mathcal{T}p).0)}\right]^2}{[1 + 0]^2}\right\}\right)$$

$$\varphi(G(p, \mathcal{T}p, \mathcal{T}p)) \leq \beta\varphi(G(p, \mathcal{T}p, \mathcal{T}p))$$

Since, $\varphi(t) \leq t$, for all $t \geq 0$.

$$G(p, \mathcal{T}p, \mathcal{T}p) \leq \beta G(p, \mathcal{T}p, \mathcal{T}p)$$

which is contradiction, since $\beta < 1$

$$Hence,\ \mathcal{T}p = p \tag{3.14}$$

Using 3.1 and rectangular inequality in def. 2.1, we obtain p is the unique fixed point of $\mathcal{T}$ by Theorem 3.1.

To prove: $\{u_n\}$ converging to p in $\mathcal{X}$.

Consider,

$$\begin{aligned}\varphi(G(p, u_n, u_n)) &= \varphi(G(\mathcal{T}u, u_n, u_n)) \\ &\leq \varphi(G(u_{n+1}, u_n, u_n)) + \varphi(G(\mathcal{T}u, u_{n+1}, u_{n+1})) \\ &\leq \varphi(G(u_{n+1}, u_n, u_n)) + \alpha\varphi(G(p, u_n, u_n)) + \beta\varphi\left(\max\{G(u_{n+1}, u_{n+1}, u_n), G(p, u_n, u_n)\}\right) \\ &+ \gamma\varphi\left(\left\{\frac{G(p, u_n, u_n)\left[1 + \sqrt{G(u_{n+1}, u_{n+1}, u_n).G(p, u_n, u_n)}\right]^2}{[1 + G(p, u_n, u_n)]^2}\right\}\right)\end{aligned}$$

Using condition (3.4), we get

$$\begin{aligned}\varphi(G(p, u_n, u_n)) &\leq 0 + \alpha\varphi(G(p, u_n, u_n)) + \beta\varphi\left(\max\{G(0), G(p, u_n, u_n)\}\right) \\ &+ \gamma\varphi\left(\left\{\frac{G(p, u_n, u_n)\left[1 + \sqrt{(0).G(p, u_n, u_n))}\right]^2}{[1 + G(p, u_n, u_n)]^2}\right\}\right)\end{aligned}$$

$$\leq \alpha\varphi(G(p,u_n,u_n)) + \beta\varphi(G(p,u_n,u_n)) + \gamma\varphi(G(p,u_n,u_n))$$

$$\varphi(G(p,u_n,u_n)) \leq (\alpha+\beta+\gamma)\varphi(G(p,u_n,u_n))$$

Since, $\varphi(t) \leq t$, for all $t \geq 0$

$$G(p,u_n,u_n) \leq \mathcal{L}G(p,u_n,u_n)$$

$$G(p,u_n,u_n) - \mathcal{L}G(p,u_n,u_n) = 0$$

$$G(p,u_n,u_n) = 0$$

$$\lim_{n\to\infty} G(p,u_n,u_n) = 0 \tag{3.15}$$

Thus, $\{u_n\}$ converging to p in $\mathcal{X}$. □

Corollary 3.2. *In a complete symmetric G-metric space* $(\mathcal{X}, G)$, *a self mapping* $\mathcal{T} : \mathcal{X} \to \mathcal{X}$ *has a unique fixed point and also* $\{u_n\}$ *converging to a point* $p \in \mathcal{X}$ *if there exists a comparison function and* $\{u_n\}$ *has a subsequence converging to a point* $p \in \mathcal{X}$ *with for all* $x, y \in \mathcal{X}$,

$$\begin{aligned}\varphi(G(\mathcal{T}x,\mathcal{T}y,\mathcal{T}x)) \leq{}& \alpha\varphi(G(x,y,x)) + \beta\varphi\left(\max\{G(x,\mathcal{T}x,\mathcal{T}x), G(x,y,x)\}\right)\\ &+ \gamma\varphi\left(\left\{\frac{G(x,y,x)\left[1+\sqrt{G(x,\mathcal{T}x,\mathcal{T}x).G(x,y,x)}\right]^2}{[1+G(x,y,x)]^2}\right\}\right)\end{aligned} \tag{3.16}$$

where $\alpha, \beta, \gamma \in [0,1)$ *and* $0 \leq \mathcal{L} = \alpha+\beta+\gamma < 1$.

Proof. Put $x = z$, we get the conclusion by using Theorem 3.2. □

4. Application of Proposed G-metric Space Based Image Contraction Algorithm

Any grayscale digital image can be figured off as a matrix, with each element indicating the pixel's grey value in the corresponding index. Rectangular arrays of square pixels are used to represent digital images. These pixels have 256 shades [0, 255] in gray scale, 8 but, with 0 being black and 255 being white, and 254 shades of grey in between. As described in the following algorithm, the methodology involves parallel local operations on each element (pixel value) and immediate states.

Step 1: Place the grayscale image $\mathcal{I}$ into the programme.

Step 2: From $\mathcal{I}$, get matrix $\mathcal{A}$ of order $p \times q$.

Step 3: Divide the space into fixed-size blocks $N = n \times n (n \geq 2)$.

Step 4: Using extend G- contraction condition, find the $\mathcal{B}_s^1$ that corresponds to each $\mathcal{A}_s^n$.

Step 5: Obtain matrix $\mathcal{B}$, which has been contracted.

Step 6: Get the image $\mathcal{I}'$ that was contracted.

For the implementation of the above algorithm, the authors used matlab. The intensity of each pixel in the image is used as a starting point, and each element of $\mathcal{I}$ is transformed into a matrix representing that pixel's intensity. Divide $\mathcal{I}$ into several fixed-block-size segments, below are the pixel values for the illustrated box in Fig. 1, as well as the contracted region that was considered. As an outcome, the pixel values will differ according to the size of the contracted part. For the depicted region,

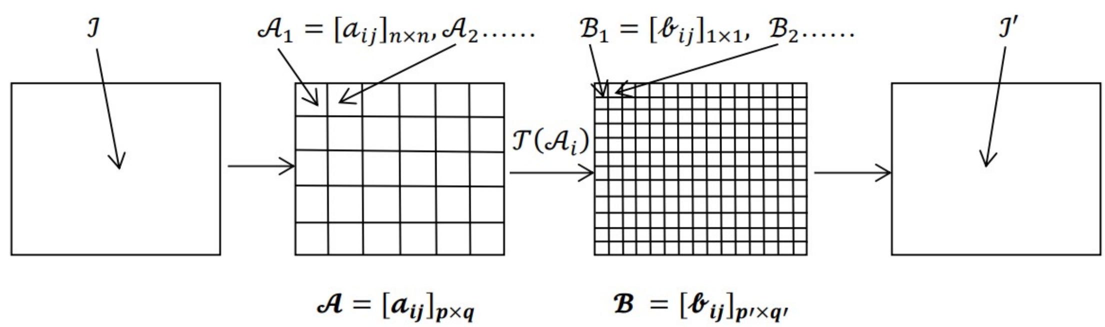

Figure 1. The above figure to show steps of scheme

Define a mapping $\mathcal{T} : \mathcal{A} \to \mathcal{A}$ given as:

$$\mathcal{T}(\mathcal{A}_i) = \max\{\mathcal{A}_i : \mathcal{A}_i \in \mathcal{A}\} \tag{4.1}$$

Each $N = n \times n$ is a non-overlapping square sub-matrix $\mathcal{A}_s^n$ of fixed dimension ($n \geq 2$), resulting in $\mathcal{A} = \cup_{i=1}^{s} \mathcal{A}_s^n$. Using the function $\mathcal{T}$ is maximum values, each one of $\mathcal{A}_s^n$ is changed to a square sub-matrix $\mathcal{B}_s^1$ of dimension 1×1. All these $\mathcal{B}_s^1$ matrices are sequentially positioned in place $\mathcal{A}_s^n$ of each to produce a contracted matrix with a smaller dimension than the initial matrix $\mathcal{A}$. Convert contracted matrix $\mathcal{B}$ to contracted image $\mathcal{I}'$, which takes up less space than $\mathcal{I}$.

5. Proposed Approach

Initially, consider the different resolution of images such as low resolution images and high resolution images.

5.1. Low Resolution Images. The low resolution images are ship, chest and flower of grayscale image of region space of 512×512, 720×820 and 600×471 respectively. We will focus on a limited 16×16 region, as shown by an illustrated small circle in Figs. 2, 3 and 4, each block is handled independently of the others.

Figure 2. 512 × 512

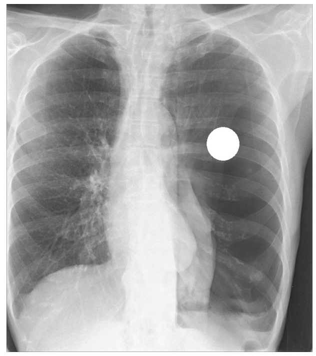

Figure 3. 720 × 820

Figure 4. 600 × 471

5.2. **High Resolution Images.** The high resolution images are satellite, paddy field and stadium of grayscale image of region space of 1200 × 720, 1280 × 1024 and 1920 × 1200 respectively. We will focus on a limited 16 × 16 region, as shown by an illustrated small circle in Figs. 5, 6 and 7, each block is handled independently of the others.

Figure 5. 1200 × 720

Figure 6. 1280 × 1024

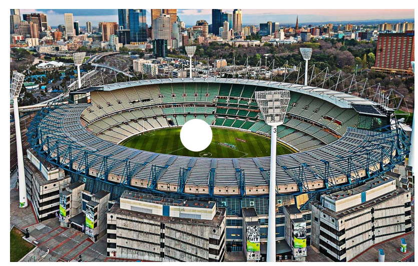

Figure 7. 1920 × 1200

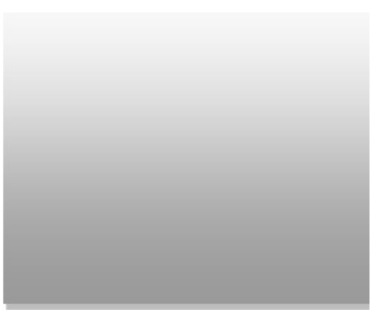

Figure 8. Sub matrix (16 × 16)

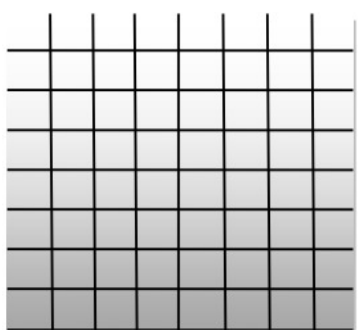

Figure 9. 64 $\mathcal{A}_s^2$ 2 × 2

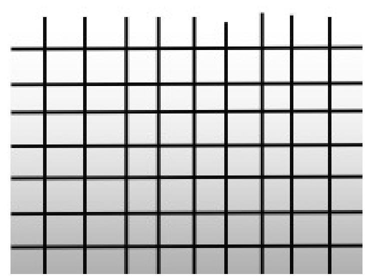

Figure 10. 64 $\mathcal{B}_s^1$ 1 × 1

Fig. 8 shows that, the 16 × 16 region blown up to emphasize the independent pixels, whereas Fig. 9 and Fig. 10 show the subdivision corresponding to 64 non-overlapping $\mathcal{A}_s^2$, each of which is a

2×2 block, and 64 non-overlapping $\mathcal{B}_s^1$, each of which is a 1×1 block. Below are the pixel values for the highlighted box in Fig. 8 and the contracted region when considering $\mathcal{A}_s^n$ for $n = 2$. For $n > 2$, as a result of the varying pixel values, the contracted region's size will vary. In the region illustrated,

$$\mathcal{A} = \begin{bmatrix} 127 & 123 & 125 & 120 & 126 & 123 & 127 & 128 & 125 & 129 & 129 & 132 & 129 & 132 & 127 & 120 \\ 128 & 126 & 128 & 122 & 125 & 125 & 122 & 129 & 127 & 128 & 131 & 128 & 129 & 131 & 128 & 127 \\ 128 & 124 & 128 & 126 & 127 & 120 & 128 & 129 & 128 & 131 & 135 & 126 & 130 & 126 & 128 & 129 \\ 124 & 127 & 128 & 129 & 121 & 128 & 129 & 128 & 129 & 133 & 130 & 132 & 128 & 130 & 128 & 125 \\ 126 & 125 & 128 & 126 & 126 & 125 & 127 & 128 & 131 & 127 & 128 & 136 & 127 & 128 & 130 & 129 \\ 125 & 127 & 126 & 126 & 128 & 128 & 128 & 126 & 130 & 129 & 128 & 131 & 132 & 128 & 130 & 131 \\ 127 & 127 & 128 & 124 & 120 & 127 & 128 & 126 & 128 & 131 & 134 & 127 & 128 & 128 & 128 & 130 \\ 123 & 135 & 120 & 128 & 121 & 123 & 126 & 126 & 128 & 133 & 131 & 129 & 131 & 129 & 130 & 131 \\ 126 & 128 & 124 & 128 & 125 & 123 & 128 & 130 & 128 & 132 & 128 & 131 & 129 & 132 & 127 & 128 \\ 124 & 128 & 127 & 124 & 127 & 121 & 128 & 130 & 132 & 133 & 133 & 128 & 128 & 129 & 130 & 133 \\ 122 & 126 & 128 & 126 & 123 & 127 & 124 & 129 & 131 & 134 & 130 & 130 & 129 & 133 & 126 & 131 \\ 126 & 127 & 125 & 122 & 125 & 121 & 127 & 128 & 131 & 131 & 132 & 129 & 131 & 131 & 134 & 128 \\ 122 & 128 & 133 & 120 & 126 & 125 & 125 & 128 & 135 & 127 & 132 & 128 & 127 & 129 & 128 & 128 \\ 123 & 128 & 127 & 122 & 125 & 126 & 130 & 124 & 131 & 130 & 132 & 132 & 129 & 130 & 132 & 127 \\ 122 & 127 & 128 & 126 & 126 & 127 & 125 & 128 & 130 & 129 & 132 & 133 & 129 & 132 & 133 & 129 \\ 124 & 125 & 132 & 120 & 132 & 124 & 128 & 127 & 128 & 131 & 132 & 129 & 129 & 132 & 129 & 128 \end{bmatrix}$$

$$\mathcal{T}(\mathcal{A}) = \begin{bmatrix} 128 & 128 & 126 & 129 & 129 & 132 & 132 & 128 \\ 128 & 129 & 128 & 129 & 133 & 135 & 130 & 129 \\ 127 & 128 & 128 & 128 & 131 & 136 & 132 & 131 \\ 135 & 128 & 127 & 128 & 133 & 134 & 131 & 131 \\ 128 & 128 & 127 & 130 & 133 & 133 & 132 & 133 \\ 127 & 128 & 127 & 129 & 134 & 132 & 133 & 134 \\ 128 & 133 & 126 & 130 & 135 & 132 & 130 & 132 \\ 127 & 132 & 132 & 128 & 131 & 133 & 132 & 133 \end{bmatrix}$$

For extend G- contraction condition (3.1),

$$\begin{aligned} \varphi(G(\mathcal{T}(\mathcal{A}_1), \mathcal{T}(\mathcal{A}_2), \mathcal{T}(\mathcal{A}_3))) \leq \alpha\varphi(G(\mathcal{A}_1, \mathcal{A}_2, \mathcal{A}_3)) + \beta\varphi\left(\max\left\{G(\mathcal{T}(\mathcal{A}_1), \mathcal{A}_1, \mathcal{T}(\mathcal{A}_1)), G(\mathcal{A}_1, \mathcal{A}_2, \mathcal{A}_3)\right\}\right) \\ + \gamma\varphi\left(\left\{\frac{G(\mathcal{A}_1, \mathcal{A}_2, \mathcal{A}_3)\left[1 + \sqrt{G(\mathcal{T}(\mathcal{A}_1), \mathcal{A}_1, \mathcal{T}(\mathcal{A}_1)).G(\mathcal{A}_1, \mathcal{A}_2, \mathcal{A}_3)}\right]^2}{[1 + G(\mathcal{A}_1, \mathcal{A}_2, \mathcal{A}_3)]^2}\right\}\right) \end{aligned} \tag{5.1}$$

where, φ is comparison function with $\alpha, \beta, \gamma \in [0, 1)$ and $0 \leq \mathcal{L} = \alpha + \beta + \gamma < 1$.
The comparison function $\varphi : [0, \infty) \to [0, \infty)$ is defined by

$$\varphi(t) = \frac{t}{2t + 100}, t \geq 0 \tag{5.2}$$

Let $(\mathcal{A}, G)$ be a $G-$metric space and define $G : \mathcal{A} \times \mathcal{A} \times \mathcal{A} \to \mathcal{A}$ by

$$G(\mathcal{A}_1, \mathcal{A}_2, \mathcal{A}_3) = d(\mathcal{A}_1, \mathcal{A}_2) + d(\mathcal{A}_2, \mathcal{A}_3) + d(\mathcal{A}_3, \mathcal{A}_1) \tag{5.3}$$

d= Matrix distance function is taken as Forbenius norm (def. 2.4)
where,

$$d(\mathcal{A}, \mathcal{B}) = \sqrt{trace\{(\mathcal{A} - \mathcal{B})(\mathcal{A} - \mathcal{B})'\}} \tag{5.4}$$

6. Results and Analysis of Image Contraction

6.1. Low Resolution Images.

The reference of low resolution images has been reduced in size to its original size, as shown in Figs. 2, 3 and 4.

6.1.1. Ship Image: (512 × 512).

The reference of ship image has been reduced in size to its original size, as shown in Fig. 2, while the obtained contracted images are shown in Figs. 11, 12, 13 and 14.

$$Let\ \mathcal{A}_1 = \begin{bmatrix} 129 & 107 \\ 134 & 119 \end{bmatrix}, \mathcal{A}_2 = \begin{bmatrix} 102 & 104 \\ 105 & 125 \end{bmatrix} and\ \mathcal{A}_3 = \begin{bmatrix} 132 & 169 \\ 149 & 191 \end{bmatrix}$$

$$G(\mathcal{T}(\mathcal{A}_1), \mathcal{T}(\mathcal{A}_2), \mathcal{T}(\mathcal{A}_3)) = 132 \tag{6.1}$$

$$G(\mathcal{A}_1, \mathcal{A}_2, \mathcal{A}_3) = 243.33 \tag{6.2}$$

$$G(\mathcal{T}(\mathcal{A}_1), \mathcal{A}_1, \mathcal{T}(\mathcal{A}_1)) = 62.58 \tag{6.3}$$

Substitute (6.1), (6.2) and (6.3) in (5.1), we have

$$\varphi(132) \leq \alpha\varphi(243.33) + \beta\varphi(243.33) + \gamma\varphi(63.08)$$

$$0.36 \leq (\alpha + \beta)(0.41) + \gamma(0.28) \qquad (using\ (5.2)) \tag{6.4}$$

For some $\alpha, \beta, \gamma \in [0, 1)$ in (6.4) satisfies the contractivity condition (5.1).

Figure 11. 256×256

Figure 12. 170×170

Figure 13. 128×128

Figure 14. 102×102

Table 1. Summary of Original Image 2 After Contracted

	Test Image	**Contracted**			
Figure	2	11	12	13	14
Dimension	512×512	256×256	170×170	128×128	102×102
Size (KB)	256	9.75	5.59	3.45	2.58
Block Size	-	2×2	3×3	4×4	5×5
% Space Saved	-	96.19	97.82	98.65	98.99

6.1.2. **Chest Image:** (720×820). The reference of chest image has been reduced in size to its original size, as shown in Fig. 3, while the obtained contracted images are shown in Figs. 15, 16, 17 and 18.

$$Let\ \mathcal{A}_1 = \begin{bmatrix} 161 & 162 \\ 162 & 166 \end{bmatrix},\ \mathcal{A}_2 = \begin{bmatrix} 162 & 167 \\ 166 & 167 \end{bmatrix}\ and\ \mathcal{A}_3 = \begin{bmatrix} 171 & 174 \\ 170 & 176 \end{bmatrix}$$

$$G(\mathcal{T}(\mathcal{A}_1), \mathcal{T}(\mathcal{A}_2), \mathcal{T}(\mathcal{A}_3)) = 20 \tag{6.5}$$

$$G(\mathcal{A}_1, \mathcal{A}_2, \mathcal{A}_3) = 41.83 \tag{6.6}$$

$$G(\mathcal{T}(\mathcal{A}_1), \mathcal{A}_1, \mathcal{T}(\mathcal{A}_1)) = 15.10 \tag{6.7}$$

Substitute (6.5), (6.6) and (6.7) in (5.1), we have

$$\varphi(20) \leq \alpha\varphi(41.83) + \beta\varphi(41.83) + \gamma\varphi(15.57)$$

$$0.14 \leq (\alpha + \beta)(0.28) + \gamma(0.12) \qquad (using\ (5.2)) \tag{6.8}$$

For some $\alpha, \beta, \gamma \in [0, 1)$ in (6.8) satisfies the contractivity condition (5.1).

Figure 15. 410 × 410

Figure 16. 273 × 273

Figure 17. 205× 205

Figure 18. 164× 164

Table 2. Summary of Original Image 3 After Contracted

	Test Image	Contracted			
Figure	3	15	16	17	18
Dimension	720 × 820	410 × 410	273 × 273	205 × 205	164 × 164
Size (KB)	65.2	18.5	9.6	6.2	4.4
Block Size	-	2 × 2	3 × 3	4 × 4	5 × 5
% Space Saved	-	72.0	85.2	90.4	93.2

6.1.3. **Flower Image:** (600×471). The reference of flower image has been reduced in size to its original size, as shown in Fig. 4, while the obtained contracted images are shown in Figs. 19, 20, 21 and 22.

$$Let\ \mathcal{A}_1 = \begin{bmatrix} 47 & 42 \\ 49 & 46 \end{bmatrix},\ \mathcal{A}_2 = \begin{bmatrix} 67 & 39 \\ 63 & 28 \end{bmatrix} and\ \mathcal{A}_3 = \begin{bmatrix} 46 & 55 \\ 41 & 56 \end{bmatrix}$$

$$G(\mathcal{T}(\mathcal{A}_1), \mathcal{T}(\mathcal{A}_2), \mathcal{T}(\mathcal{A}_3)) = 36 \tag{6.9}$$

$$G(\mathcal{A}_1, \mathcal{A}_2, \mathcal{A}_3) = 93.09 \tag{6.10}$$

$$G(\mathcal{T}(\mathcal{A}_1), \mathcal{A}_1, \mathcal{T}(\mathcal{A}_1)) = 15.77 \tag{6.11}$$

Substitute (6.9), (6.10) and (6.11) in (5.1), we have

$$\varphi(36) \leq \alpha\varphi(93.09) + \beta\varphi(93.09) + \gamma\varphi(16.24)$$

$$0.21 \leq (\alpha+\beta)(0.33) + \gamma(0.12) \qquad (using\ (5.2)) \tag{6.12}$$

For some $\alpha, \beta, \gamma \in [0, 1)$ in (6.12) satisfies the contractivity condition (5.1).

Figure 19. 235 × 235

Figure 20. 157 × 157

Figure 21. 117× 117

Figure 22. 102× 102

Table 3. Summary of Original Image 4 After Contracted

	Test Image	Contracted			
Figure	4	19	20	21	22
Dimension	600 × 471	235 × 235	157 × 157	117 × 117	102 × 102
Size (KB)	28.9	9.2	5.2	3.5	2.6
Block Size	-	2 × 2	3 × 3	4 × 4	5 × 5
% Space Saved	-	68.9	82.0	87.8	91.0

6.2. **High Resolution Images.** The reference of high resolution images has been reduced in size to its original size, as shown in Figs. 5, 6 and 7.

6.2.1. **Satellite Image:** (1200 × 720). The reference of satellite image has been reduced in size to its original size, as shown in Fig. 5, while the obtained contracted images are shown in Figs. 23, 24, 25 and 26.

$$Let\ \mathcal{A}_1 = \begin{bmatrix} 129 & 127 \\ 119 & 131 \end{bmatrix},\ \mathcal{A}_2 = \begin{bmatrix} 126 & 136 \\ 126 & 130 \end{bmatrix} and\ \mathcal{A}_3 = \begin{bmatrix} 130 & 131 \\ 136 & 144 \end{bmatrix}$$

$$G(\mathcal{T}(\mathcal{A}_1), \mathcal{T}(\mathcal{A}_2), \mathcal{T}(\mathcal{A}_3)) = 26 \tag{6.13}$$

$$G(\mathcal{A}_1, \mathcal{A}_2, \mathcal{A}_3) = 51.98 \tag{6.14}$$

$$G(\mathcal{T}(\mathcal{A}_1), \mathcal{A}_1, \mathcal{T}(\mathcal{A}_1)) = 25.62 \tag{6.15}$$

Substitute (6.13), (6.14) and (6.15) in (5.1), we have

$$\varphi(26) \leq \alpha\varphi(51.98) + \beta\varphi(51.98) + \gamma\varphi(26.03)$$

$$0.17 \leq (\alpha + \beta)(0.25) + \gamma(0.17) \qquad (using\ (5.2)) \tag{6.16}$$

For some $\alpha, \beta, \gamma \in [0, 1)$ in (6.16) satisfies the contractivity condition (5.1).

Figure 23. 385 × 385

Figure 24. 256 × 256

Figure 25. 192× 192

Figure 26. 154× 154

Table 4. Summary of Original Image 5 After Contracted

	Test Image	**Contracted**			
Figure	5	23	24	25	26
Dimension	1200 × 720	385 × 385	256 × 256	192 × 192	154 × 154
Size (KB)	313	49.5	23.2	13.7	9.5
Block Size	-	2 × 2	3 × 3	4 × 4	5 × 5
% Space Saved	-	84.1	92.5	95.6	96.9

6.2.2. **Paddy Field Image:** (1280 × 1024). The reference of paddy field image has been reduced in size to its original size, as shown in Fig. 6, while the obtained contracted images are shown in Figs. 27, 28, 29 and 30.

$$Let\ \mathcal{A}_1 = \begin{bmatrix} 82 & 86 \\ 81 & 86 \end{bmatrix},\ \mathcal{A}_2 = \begin{bmatrix} 89 & 92 \\ 89 & 92 \end{bmatrix} and\ \mathcal{A}_3 = \begin{bmatrix} 93 & 93 \\ 93 & 93 \end{bmatrix}$$

$$G(\mathcal{T}(\mathcal{A}_1), \mathcal{T}(\mathcal{A}_2), \mathcal{T}(\mathcal{A}_3)) = 14 \tag{6.17}$$

$$G(\mathcal{A}_1, \mathcal{A}_2, \mathcal{A}_3) = 38.48 \tag{6.18}$$

$$G(\mathcal{T}(\mathcal{A}_1), \mathcal{A}_1, \mathcal{T}(\mathcal{A}_1)) = 12.80 \tag{6.19}$$

Substitute (6.17), (6.18) and (6.19) in (5.1), we have

$$\varphi(14) \leq \alpha\varphi(38.48) + \beta\varphi(38.48) + \gamma\varphi(13.27)$$

$$0.11 \leq (\alpha + \beta)(0.22) + \gamma(0.10) \qquad (using\ (5.2)) \tag{6.20}$$

For some $\alpha, \beta, \gamma \in [0, 1)$ in (6.20) satisfies the contractivity condition (5.1).

Figure 27. 512 × 512

Figure 28. 341 × 341

Figure 29. 256× 256

Figure 30. 204× 204

Table 5. Summary of Original Image 6 After Contracted

	Test Image	**Contracted**			
Figure	6	27	28	29	30
Dimension	1280 × 1280	512 × 512	341 × 341	256 × 256	204 × 204
Size (KB)	1000	53.3	24.1	13.5	9.1
Block Size	-	2 × 2	3 × 3	4 × 4	5 × 5
% Space Saved	-	94.6	97.5	98.6	99.0

6.2.3. **Stadium Image:** (1920 × 1200). The reference of stadium image has been reduced in size to its original size, as shown in Fig. 7, while the obtained contracted images are shown in Figs. 31, 32, 33 and 34.

$$Let\ \mathcal{A}_1 = \begin{bmatrix} 230 & 208 \\ 218 & 237 \end{bmatrix},\ \mathcal{A}_2 = \begin{bmatrix} 150 & 167 \\ 197 & 173 \end{bmatrix}\ and\ \mathcal{A}_3 = \begin{bmatrix} 219 & 177 \\ 210 & 188 \end{bmatrix}$$

$$G(\mathcal{T}(\mathcal{A}_1), \mathcal{T}(\mathcal{A}_2), \mathcal{T}(\mathcal{A}_3)) = 80 \tag{6.21}$$

$$G(\mathcal{A}_1, \mathcal{A}_2, \mathcal{A}_3) = 244.38 \tag{6.22}$$

$$G(\mathcal{T}(\mathcal{A}_1), \mathcal{A}_1, \mathcal{T}(\mathcal{A}_1)) = 70.74 \tag{6.23}$$

Substitute (6.21), (6.22) and (6.23) in (5.1), we have

$$\varphi(80) \leq \alpha\varphi(244.38) + \beta\varphi(244.38) + \gamma\varphi(71.23)$$

$$0.31 \leq (\alpha + \beta)(0.42) + \gamma(0.29) \qquad (using\ (5.2)) \tag{6.24}$$

For some $\alpha, \beta, \gamma \in [0, 1)$ in (6.24) satisfies the contractivity condition (5.1).

Figure 31. 600 × 600

Figure 32. 400 × 400

Figure 33. 300× 300

Figure 34. 240× 240

Table 6. Summary of Original Image 7 After Contracted

	Test Image	**Contracted**			
Figure	7	31	32	33	34
Dimension	1920 × 1200	600 × 600	400 × 400	300 × 300	240 × 240
Size (KB)	893	135	63.2	37.5	24
Block Size	-	2 × 2	3 × 3	4 × 4	5 × 5
% Space Saved	-	84.8	92.9	95.8	97.3

7. Conclusion

The notion of extended G-contraction mapping was implemented in this paper. The metric is appropriately formed in a nonempty space, and its application to use in a digital image is demonstrated. The original image size has been reduced without significant loss of image quality. As a result, the contracted image that occupied less storage space, and it is also easier to send. The framework is implemented with a variety of block sizes to see how far an image can be contracted. Since the designed function iterates repeatedly on the input image, the concluding contracted images are of high quality when the input image is exceptionally large or has little color variation.

Conflicts of Interest: The authors declare that there are no conflicts of interest regarding the publication of this paper.

References

[1] S. Banach, Sur les Opérations dans les Ensembles Abstraits et Leur Application aux Équations Intégrales, Fundam. Math. 3 (1922), 133–181.

[2] S. Gähler, 2-Metrische Räume und Ihre Topologische Struktur, Math. Nachr. 26 (1963), 115–148. https://doi.org/10.1002/mana.19630260109.

[3] B.C. Dhage, A New Approach to Generalized Metric Spaces, PhD Thesis, Marathwada, Aurangabad, India, (1963).

[4] Z. Mustafa, B. Sims, Some Remarks Concerning D-Metric Spaces, In: Proceedings of the International Conferences on Fixed Point Theory and Applications, Valencia, Spain, (2003), 189–198.

[5] Z. Mustafa, B. Sims, A New Approach to Generalized Metric Spaces, J. Nonlinear Convex Anal. 7 (2006), 289–297.

[6] Z. Mustafa, B. Sims, Fixed Point Theorems for Contractive Mappings in Complete G-Metric Spaces, Fixed Point Theory Appl. 2009 (2009), 917175. https://doi.org/10.1155/2009/917175.

[7] L.G. Huang, X. Zhang, Cone Metric Spaces and Fixed Point Theorems of Contractive Mappings, J. Math. Anal. Appl. 332 (2007), 1468–1476. https://doi.org/10.1016/j.jmaa.2005.03.087.

[8] A. Azam, B. Fisher, M. Khan, Common Fixed Point Theorems in Complex Valued Metric Spaces, Numer. Funct. Anal. Optim. 32 (2011), 243–253. https://doi.org/10.1080/01630563.2011.533046.

[9] A. Rosenfeld, Digital Topology, Amer. Math. Mon. 86 (1979), 621–630. https://doi.org/10.1080/00029890.1979.11994873.

[10] S. Han, Connected Sum of Digital Closed Surfaces, Inform. Sci. 176 (2006), 332–348. https://doi.org/10.1016/j.ins.2004.11.003.

[11] O. Ege, I. Karaca, Lefschetz Fixed Point Theorem for Digital Images, Fixed Point Theory Appl. 2013 (2013), 253. https://doi.org/10.1186/1687-1812-2013-253.

[12] O. Ege, I. Karaca, Banach Fixed Point Theorem for Digital Images, J. Nonlinear Sci. Appl. 08 (2016), 237–245. https://doi.org/10.22436/jnsa.008.03.08.

[13] S. Han, Banach Fixed Point Theorem From the Viewpoint of Digital Topology, J. Nonlinear Sci. Appl. 09 (2016), 895–905. https://doi.org/10.22436/jnsa.009.03.19.

[14] S. Thalapathiraj, B. Baskaran, J. Arunnehru, Novel Approach for Texture Feature Extraction and Classification of Satellite Images Using Modified Hilbert Matrix, AIP Conf. Proc. 2112 (2019), 020154. https://doi.org/10.1063/1.5112339.

[15] B. Baskaran, C. Rajesh, Fixed Point Theorems for Mapping on Complete G-Metric Space, Int. J. Innov. Res. Technol. 2 (2015), 30–33.

[16] B. Baskaran, C. Rajesh, Some Results on Fixed Points of Asymptotically Regular Mappings, Int. J. Math. Anal. 8 (2014), 2469–2474. https://doi.org/10.12988/ijma.2014.49279.

[17] I. Karaca, O. Ege, Some Results on Simplicial Homology Groups of 2D Digital Images, Int. J. Inform. Comput. Sci. 1 (2012), 198–203.

[18] A. Jawaharlalnehru, T. Sambandham, V. Sekar, et al. Target Object Detection from Unmanned Aerial Vehicle (UAV) Images Based on Improved YOLO Algorithm, Electronics. 11 (2022), 2343. https://doi.org/10.3390/electronics11152343.

[19] L. Boxer, Digitally Continuous Functions, Pattern Recognit. Lett. 15 (1994), 833–839. https://doi.org/10.1016/0167-8655(94)90012-4.

[20] L. Boxer, A Classical Constructions for the Digital Fundamental Group, J. Math. Imaging Vis. 10 (1999), 51–62. https://doi.org/10.1023/a:1008370600456.

[21] L. Boxer, Properties of Digital Homotopy, J. Math. Imaging Vis. 22 (2005), 19–26. https://doi.org/10.1007/s10851-005-4780-y.

[22] A.C.M. Ran, M.C.B. Reurings, A Fixed Point Theorem in Partially Ordered Sets and Some Applications to Matrix Equations, Proc. Amer. Math. Soc. 132 (2004), 1435–1443.

[23] Sanjay Kumar Tiwari, Himanshu Kumar Pandey, Fixed Point Theorem in S-Metric Space, PanAmer. Math. J. 31 (2021), 19–28.

[24] T.B. Singh, G.A.H. Sharma, Y.M. Singh, M.R. Singh, Common Fixed Point Theorems for Six Self-Mappings on S-Metric Spaces, Int. J. Anal. Appl. 19 (2021), 794–811. https://doi.org/10.28924/2291-8639-19-2021-794.

[25] A. Khan, P.N. Pathak, S. Sharma, G. Verma, V. Kumar, J.P. Tripathi, Fixed Point Theorems Using Comparison Functions View to Dislocated Quasi-Metric Spaces, ECS Trans. 107 (2022), 11969–11980. https://doi.org/10.1149/10701.11969ecst.

[26] J. Arunnehru, S. Thalapathiraj, R. Dhanasekar, L. Vijayaraja, R. Kannadasan, A.A. Khan, M.A. Haq, M. Alshehri, M.I. Alwanain, I. Keshta, Machine Vision-Based Human Action Recognition Using Spatio-Temporal Motion Features (STMF) with Difference Intensity Distance Group Pattern (DIDGP), Electronics. 11 (2022), 2363. https://doi.org/10.3390/electronics11152363.

[27] W. Shatanawi, A. Pitea, R. Lazović, Contraction Conditions Using Comparison Functions on b-Metric Spaces, Fixed Point Theory Appl. 2014 (2014), 135. https://doi.org/10.1186/1687-1812-2014-135.

[28] N. Hussain, Z. Kadelburg, S. Radenović, F. Al-Solamy, Comparison Functions and Fixed Point Results in Partial Metric Spaces, Abstr. Appl. Anal. 2012 (2012), 605781. https://doi.org/10.1155/2012/605781.

[29] R.K. Vats, S. Kumar, V. Sihag, Common Fixed Point Theorem For Expansive Mappings In G-metric Spaces, J. Math. Comput. Sci. 06 (2013), 60–71. https://doi.org/10.22436/jmcs.06.01.06.

[30] A. Choudhury, T. Som, Few Common Fixed Point Results For Weakly Commuting Mappings, J. Math. Comput. Sci. 06 (2013), 27–35. https://doi.org/10.22436/jmcs.06.01.04.

[31] Z. Mustafa, M.M.M. Jaradat, H.M. Jaradat, A Remarks on the Paper "Some Fixed Point Theorems for Generalized Contractive Mappings in Complete Metric Spaces", J. Math. Anal. 8 (2017), 17–22.

[32] Z. Mustafa, M.M.M. Jaradat, A. Ansari, F. Gu, H. Zheng, S. Radenović, M.S. Bataineh, Common Fixed Point Theorems for Two Pairs of Self-Mappings in Partial Metric Space Using C-Class Functions on (ψ, ϕ)-Contractive Condition, J. Math. Comput. Sci. 18 (2018), 216–231. https://doi.org/10.22436/jmcs.018.02.09.

[33] S. Vaijayanthi, J. Arunnehru, Human Emotion Recognition from Body Posture with Machine Learning Techniques, in: M. Singh, V. Tyagi, P.K. Gupta, J. Flusser, T. Ören (Eds.), Advances in Computing and Data Sciences, Springer International Publishing, Cham, 2022: pp. 231–242. https://doi.org/10.1007/978-3-031-12638-3_20.

[34] M. Kumar, S. Arora, M. Imdad, W. M. Alfaqih, Coincidence and common fixed point results via simulation functions in G-metric spaces, J. Math. Comput. Sci. 19 (2019), 288–300. https://doi.org/10.22436/jmcs.019.04.08.

[35] D. Lateef, Fisher Type Fixed Point Results in Controlled Metric Spaces, J. Math. Comput. Sci. 20 (2020), 234–240. https://doi.org/10.22436/jmcs.020.03.06.

[36] S. M. Abusalim, Z. M. Fadail, New Coupled and Common Coupled Fixed Point Results With Generalized c-Distance on Cone b-Metric Spaces, J. Math. Comput. Sci. 25 (2021), 209–218. https://doi.org/10.22436/jmcs.025.03.01.

[37] A. El Haddouchi, B. Marzouki, A generalized fixed point theorem in G-metric space, J. Anal. Appl. 17 (2019), 89–105.

[38] N. Kumar, M. Kumar, Ashish, Fixed Point Theory for Simulation Functions in G-Metric Spaces: A Novel Approach, Adv. Fixed Point Theory, 12 (2022), 5. https://doi.org/10.28919/afpt/7256.

[39] S. Koirala, N.P. Pahari, Some Results on Fixed Point Theory in G–metric Space, Int. J. Math. Trends Technol. 67 (2021), 150–156. https://doi.org/10.14445/22315373/ijmtt-v67i5p516.

[40] G. Bhargavi, J. Arunnehru, Deep Learning Framework for Landslide Severity Prediction and Susceptibility Mapping, Intell. Autom. Soft Comput. 36 (2023), 1257–1272. https://doi.org/10.32604/iasc.2023.034335.